The Selective Formation of Di-σ N−Si Linkages in Pyrazine Binding on Si(111)-7 × 7

Hai Gou Huang, Zhong Hai Wang, and Guo Qin Xu*

Department of Chemistry, National University of Singapore, 10 Kent Ridge, Singapore, 119260

Received: November 12, 2003

The highly selective covalent binding of pyrazine on Si(111)-7 × 7 has been investigated using high-resolution electron energy loss spectroscopy (HREELS), X-ray photoelectron spectroscopy (XPS), and density functional theory (DFT) calculations. HREELS results clearly suggest that covalently attached pyrazine retains the sp^2 electronic configuration for all four carbon atoms, indicating that the carbon atoms of the ring are not directly involved in the chemical binding with the surface. The vibrational results further reveal that the aromatic ring of pyrazine is transformed to an unconjugated cyclodiene structure, implying the participation of N atoms in surface binding. This is further confirmed by the binding energy of N 1s shifting to 399.0 eV in chemically bonded pyrazine compared to the value of 400.6 eV for physisorbed molecules. These experimental results coupled with our theoretical DFT calculations strongly suggest the di-σ binding of the two para nitrogen atoms of pyrazine with an adjacent adatom−rest-atom pair on Si (111)-7 × 7, forming a 1,4-*N*,*N*-dihydropyrazine-like structure.

I. Introduction

The covalent binding of organic molecules on semiconductor surfaces has been attracting much attention recently due to its fundamental scientific significance as well as potential applications in functional devices, such as chemical and biological sensors and molecular electronics.[1−3] Since the function and performance of these devices are inevitably related to the physical and chemical properties of the organic/semiconductor interfaces, fundamental research on interfacial and surface chemistry of semiconductors is expected to provide useful information and knowledge for designing and creating new Si-based devices as well as significantly fostering the development of molecular electronics and its related fields.

Among the silicon single-crystal surfaces, of great fundamental interests is Si(111)-7 × 7. Its structure is schematically shown in Figure 1 based on the dimer-adatom-stacking (DAS) faulted mode.[4,5] Because of the unique spatial arrangements of surface atoms together with redistribution of surface electrons, the surface provides a number of chemically, spatially, and electronically inequivalent reactive sites, including adatoms and rest atoms in the inherently different faulted and unfaulted halves as well as corner holes. The reactivity and reaction mechanisms of aromatic molecules with the Si dangling bonds of Si (111)-7 × 7 have been explored.[6−11] For five-membered heterocyclic molecules, thiophene[6] and furan[7] react with the adjacent adatom−rest atom pair through their two α-carbon atoms to form C−Si σ linkages, denoted as a [4 + 2]-like cycloaddition ("4" refers to the number of participating adsorbate atoms inside the resulting adduct ring upon adsorption, and the "2" simply refers to the two participating surface atoms, which may or may not be adjacent to each other). In the case of pyrrole, the dissociative adsorption via the breakage of its N−H bond was observed to be the dominant reaction channel.[8] The resulting fragments of pyrrolyl and the H atom are bonded to the adjacent adatom and the rest atom, respectively. Among the six-membered aromatic systems, benzene readily reacts with the surface reactive sites, forming a di-σ-bonded 1,4-cyclohexadiene-like surface intermediate through the [4 + 2]-like addition reaction.[9,10] Replacing one of the C atoms in the benzene ring by a N atom results in pyridine with a noneven electronic density distribution. Dative bonding between the electron-rich N atom of pyridine and electron-deficient Si adatoms was detected in addition to the di-σ binding configuration through the N atom and its opposite C atom.[11] To further understand the effect of constituent ring atoms on the reactivity, pyrazine is an interesting system for investigation.

The pyrazine ring is an important functional constituent in a variety of natural and synthetic compounds, e.g., monoucleotides.[12] It is a six-membered heteroatomic aromatic compound. All four C atoms and two N atoms take part in the large π bond formed by six conjugated 2p electrons (one from each of them). Expectably, each nitrogen atom has a lone pair of electrons that does not directly participate in the formation of the aromatic ring. These electrons are localized at the nitrogen atoms, making them electron rich. Thus, in a chemical reaction, the N atoms of pyrazine could possibly act as a donor to provide electrons to form a dative bond with electron-deficient Si dangling bonds on adatoms, similar to the interaction of pyridine on Si(100)[13] or Si(111)-7 × 7.[11] On the other hand, in view of high reactivity of aromatic molecules on Si(111)-7 × 7 through [4 + 2]-like addition, there are two possible di-σ binding schemes for pyrazine: (1) forming Si−C σ-linkages through two opposite carbon atoms of the aromatic ring and (2) involving the two para nitrogen atoms, resulting in Si−N linkages. Thus, studying the reaction of pyrazine will enable us to correlate the electronic properties of the constituent atoms of the ring with their reactivity and selectivity on Si(111)-7 × 7. This information will offer the flexibility for the modification of silicon surfaces, useful in designing the desired molecular templates.

The adsorption of pyrazine on metal surfaces, such as Ag(111) and Au(111), was extensively investigated.[14−18] The results revealed that pyrazine adsorbs flat on Ag(111) at all

* Author to whom correspondence may be addressed. Email: chmxugq@nus.edu.sg. Fax: (65) 6779 1691.

10.1021/jp037456y CCC: $27.50
Published on Web 07/22/2004

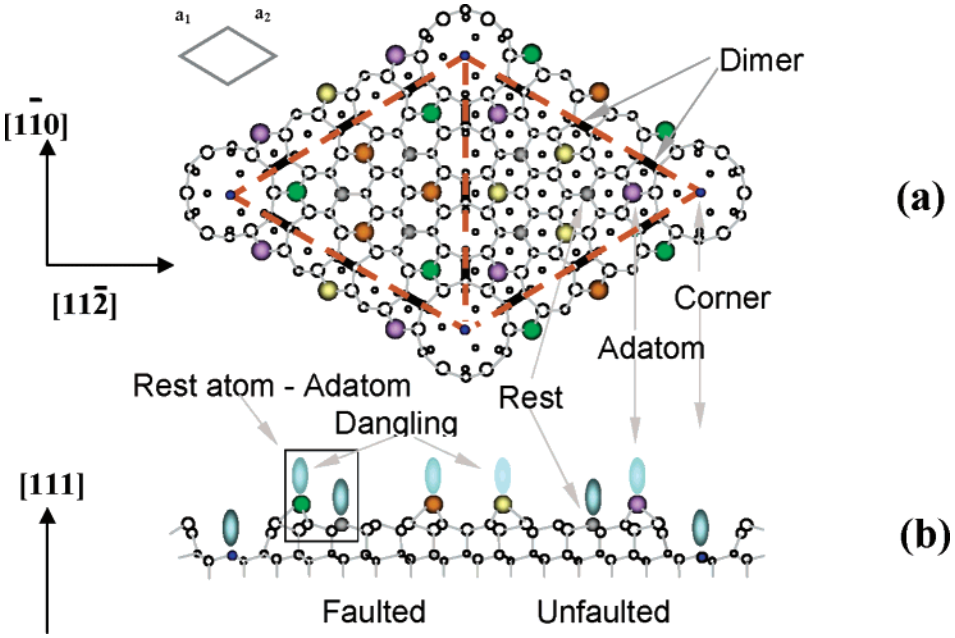

Figure 1. The top (a) and side (b) views of the detailed three-dimensional structure for one Si(111)-7 × 7 unit cell based on the DAS faulted model.

coverages, but on Au(111), its orientation displays flat-to-vertical transition with increase of surface coverage.

In the present work, the interaction of pyrazine with the silicon dangling bonds on Si(111)-7 × 7 has been studied using high resolution electron energy loss spectroscopy (HREELS), X-ray photoelectron spectroscopy (XPS), and density functional theory (DFT) calculations. Our experimental results showed that the covalent attachment of pyrazine occurs in a highly selective way through the formation of two Si−N bonds, not directly involving the carbon atoms of the ring, as evidenced in the retention of sp^2 configuration for all the carbon atoms in HREELS together with the observation of a large downshift (1.6 eV) for N 1s binding energy (BE) in the XPS studies. A model involving the two para nitrogen atoms of the aromatic ring binding with the adjacent adatom−rest-atom pair is predicted in our DFT calculations, consistent with the experimental observation.

II. Experimental Section

The experiments were performed in two separate ultrahigh vacuum chambers with a base pressure of $<2 \times 10^{-10}$ Torr, achieved with turbo-molecular and sputter-ion pumps. One of them is equipped with an X-ray gun (both Mg and Al anodes) and a hemispherical energy analyzer (CLAM 2, VG) for XPS. The other chamber mainly consists of a high-resolution electron energy loss spectrometer HREELS, LK-2000−14R and a quadruple mass spectrometer (UTI-100) for gas analysis.

For HREELS experiments, the electron beam with an energy of 5.0 eV impinges on Si(111)-7 × 7 at an incident angle of 60° with a resolution of 6−7 meV (full width at half maximum (fwhm), 55 cm^{-1}). XPS spectra were acquired using Mg Kα radiation ($h\nu = 1253.6$ eV) and a 20 eV pass energy. For XPS, the BE scale is referenced to the peak maximum of the Si 2p line (99.3 eV calibrated for Au $4f_{7/2}$)[19] of Si (111)-7 × 7 with a fwhm of less than 1.2 eV.

The samples with a dimension of 8 × 18 × 0.35 mm^3 were cut from *n*-type Si(111) wafers (*Phosphors*-doped, with a resistivity of 1−30 Ω cm, 99.999%, Goodfellow); a Ta-sheet heater (0.025 mm thick, Goodfellow) was sandwiched tightly between two Si(111) crystals held together by two Ta clips. Uniform heating of the samples was achieved by passing current through the Ta heater. This sample mounting configuration allows us to resistively heat the samples to 1400 K and conductively cool them to 110 K using liquid nitrogen. The temperature distribution on the samples is within ±10 K at 1000 K, determined using a pyrometer ($\epsilon = 0.74$, TR-630, Minolta).

The Si(111) sample was cleaned by repeated ion sputtering−annealing cycles (500 eV Ar^+ bombardment for 30 min with an ion current density of ~5 μA cm^{-2} and subsequent annealing to 1250 K for 20 min). The (7 × 7) reconstruction was formed after the final annealing procedure. The surface cleanliness was routinely monitored using XPS and HREELS. Pyrazine (Aldrich, 99.0%) and pyrazine-d_4 (Aldrich, 95.0%) were further purified by freeze−pump−thaw cycles and dosed onto Si(111)-7 × 7 through a variable leaking valve. The exposures in the unit of Langmuir (L) were calculated based on the exposure pressure and time without the calibration of ion gauge sensitivity.

III. Results

III.A. HREELS. Figure 2 shows the HREELS of Si(111)-7 × 7 exposed to pyrazine at 110 K. The vibrational frequencies and their assignments for physisorbed and chemisorbed molecules on a Si(111)-7 × 7 surface are listed in the Table 1. This table clearly shows that the vibrational features of physisorbed pyrazine (parts c, d, and e of Figure 2) are in excellent agreement with the IR spectrum of liquid pyrazine.[20,21] Among these vibrational signatures, the peak at 3071 cm^{-1} is assigned to the (sp^2) C−H stretching of the molecule. The feature at 1556 cm^{-1} is related to the conjugated C═C (N) stretching vibration.

The vibrational features of chemisorbed pyrazine taken at low exposures (Figure 2a) or obtained after annealing the multilayer pyrazine-covered sample to 300 K to drive away all the physisorbed molecules and retain only the chemisorbed molecules (Figure 2f), however, are significantly different. Losses at 497, 712, 905, 1065, 1230, 1615, and 3071 cm^{-1} can be readily resolved. Compared to physisorbed molecules, chemisorbed pyrazine does not lead to obvious variations in the

TABLE 1: Vibrational Modes Assignment for Physisorbed and Chemisorbed Pyrazine (PZ) on Si(111)-7 × 7[a]

class	description	IR liquid	physisorbed PZ/Si(111)	description	chemisorbed PZ/Si(111)	calculated vibrational frequencies for PZ/Si(111)
A2	oop[b] ring deformation	350				
B1	oop skeletal bend	418	402			
	Si−N stretch			Si−N stretch	497	503
A2	ring deformation	602				
B2	skeletal deformation	704		oop CH bend	712	728
B1	oop skeletal bend	756				
B1	oop C−H bend	785	769	oop C−H bend		834
A2	oop C−H bend	927		ring deformation	905	932
A2	oop C−H bend	960				
B1	oop C−H bend	983				
A1	ring breathing	1016				
A1	ring deformation	1018	1030			
B2	C−H bend	1063		asym ring deformation	1065	1015
A1	C−H bend	1130		sym ring deformation		1144
B2	ring deformation	1149				
A1	C−H bend	1233	1215	in plane C−H bend	1230	1267
B1	in plane (ring mode)	1346				
B2	in plane (ring mode)	1411	1408			
A1	in plane (ring mode)	1483				
B2	in plane (ring mode)	1525	1556			
A2	C=C stretch			sym C=C stretch	1615	1601
A1	C−H stretch	3012				
B2	C−H stretch	3040				3043
A1	C−H stretch	3055				3071
B2	C−H stretch	3069	3071	C−H stretch	3071	3073
						3095

[a] IR data for liquid pyrazine (ref 21) is included for comparison (the vibrational frequencies are given in cm^{-1}). [b] Out of plane.

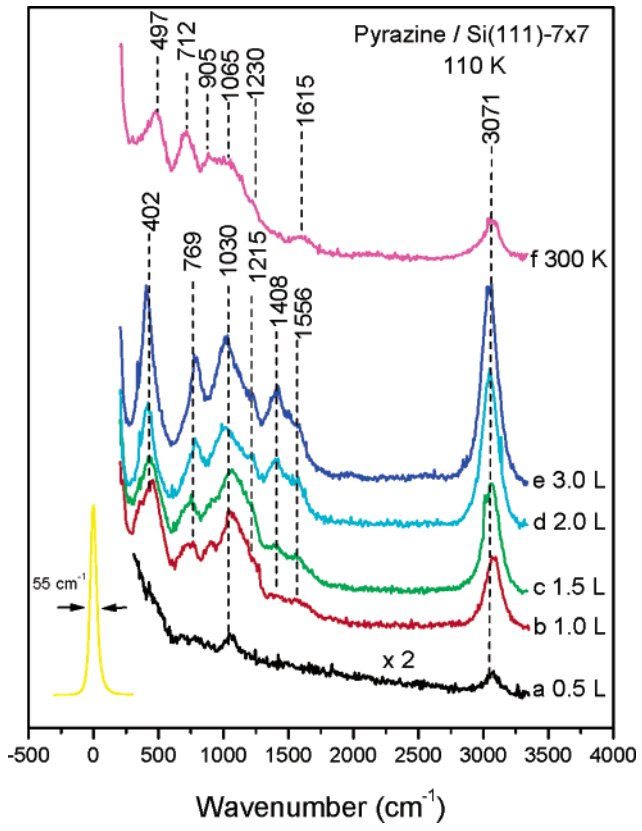

Figure 2. HREELS spectra of pyrazine Si(111)-7 × 7 as a function of exposure at 110 K. $E_p = 5.0$ eV, specular geometry. Figure 2f is the difference spectrum of saturated chemisorption monolayer.

stretching frequency of (sp^2) C−H. This result indicates that the C atoms of the molecule are not involved in the chemical binding with the surface (a (sp^3) C−H vibrational peak, redshifted by 80−100 cm^{-1} from the (sp^2) C−H stretching mode, would be expected if the C atoms were involved in binding with silicon surface dangling bonds). The 1615 cm^{-1} loss observed is attributed to the nonconjugated C=C stretching vibration in the chemisorbed pyrazine. This assignment is consistent with the results obtained for liquid 1,4-cyclohexadiene[22] (at 1639 cm^{-1}) and chemisorbed benzene[10] (at 1635 cm^{-1}) and chlorobenzene[23] (at 1628 cm^{-1}) on Si(111)-7 × 7 with a 1,4-hexadiene-like surface intermediate. On the other hand, the loss feature at 497 cm^{-1} is associated with the Si−N stretching mode, consistent with previous studies on the binding of unsaturated N-containing organic molecules on Si surfaces through the N−Si linkages.[24−26] Furthermore, we did not observe any peak at ∼2055 cm^{-1} associated with the Si−H stretching mode, [27] indicating the molecular nature of chemisorbed pyrazine on the Si(111)-7 × 7 surface. The detailed assignments are tabulated in Table 1. The main vibrational features of chemisorbed pyrazine correlates well with the calculated vibrational frequencies for chemisorbed pyrazine on Si(111)-7 × 7. The details of DFT theoretical modeling will be given in section III.C.

To further confirm our assignments, pyrazine-d_4 adsorption was also studied in our HREELS experiments. Figure 3 presents the vibrational features of physisorbed pyrazine-d_4 and the saturated chemisorption monolayer on Si(111)-7 × 7. The intensity at 2291 cm^{-1} is readily identified in the vibrational spectrum of physisorbed pyrazine-d_4 (Figure 3a) and can be attributed the (sp^2) C−D stretching, replacing the (sp^2) C−H stretching mode (at 3071 cm^{-1}) for physisorbed pyrazine (Figure 2e). Upon chemisorption (Figure 3b), the =C−D stretching frequency remains almost constant, retaining sp^2 hybridization for all four carbon atoms of the chemisorbed pyrazine on Si(111)-7 × 7. This result again shows that the C atoms do not directly bind to the silicon surface dangling bonds. In addition, the spectrum of chemisorbed pyrazine-d_4 (Figure 3b) also shows the characteristic vibrational modes of the unconjugated C=C at 1595 cm^{-1} and Si−N at 512 cm^{-1}. The absence of (sp^3) C−H (D) stretching mode, together with the formation of unconjugated C=C bond, suggests that pyrazine is directly bonded to the adjacent adatom and rest atom on Si(111)-7 × 7 through the two para nitrogen atoms, forming the two new Si−N σ linkages.

III.B. XPS. The N (1s) and C (1s) spectra of pyrazine following a sequence of exposure at 110 K are shown in Figures

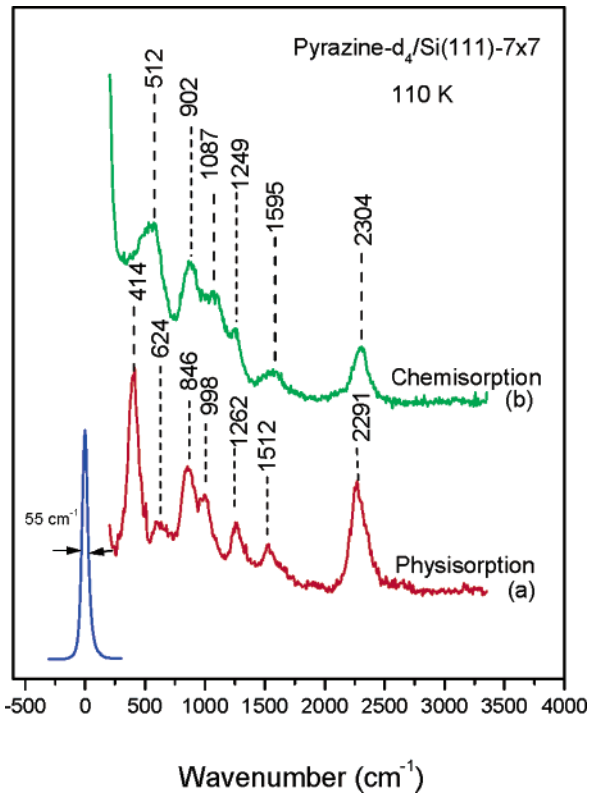

Figure 3. HREELS spectra of the physisorbed and saturated chemisorption pyrazine-d_4 on Si(111)-7 × 7.

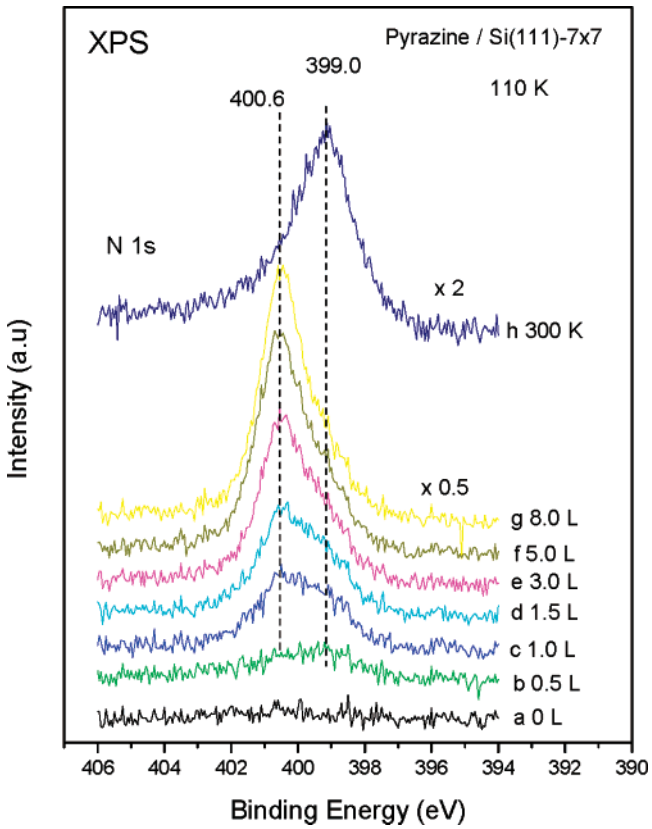

Figure 4. N 1s XPS spectra of pyrazine on Si(111)-7 × 7 at 110 K as a function of exposure. Figure 4h is the difference spectrum of saturated chemisorption monolayer.

4 and 5, respectively. At very low exposures, the N 1s spectra show a main peak centered at 399.0 eV. With an increase in the exposure from 3.0 to 8.0 L, the peak at 400.6 eV

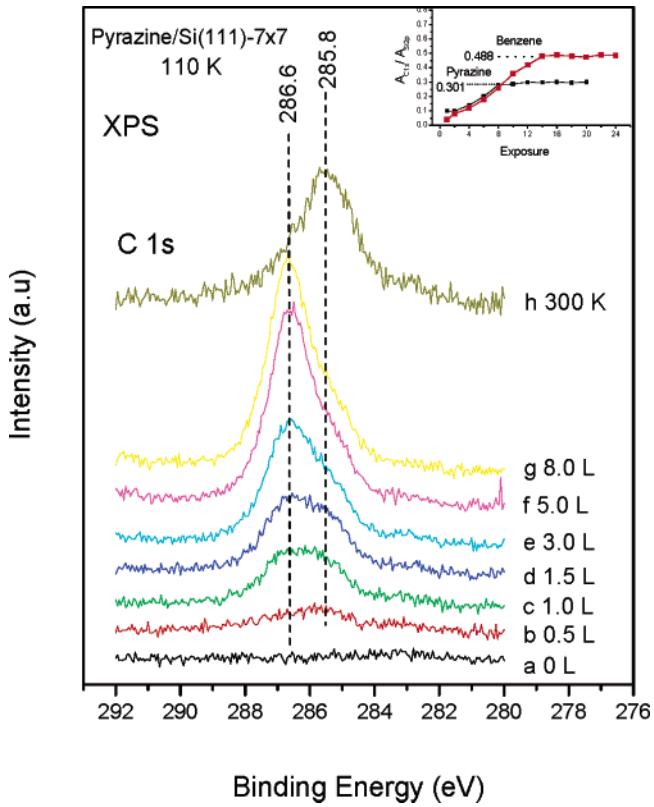

Figure 5. C 1s XPS spectra of pyrazine on Si(111)-7 × 7 at 110 K as a function of exposure. Figure 5h is the difference spectrum of saturated chemisorption monolayer. The inset plots the XPS peak area ratio, A_{C1s}/A_{Si2p}, for pyrazine and benzene on Si(111)-7 × 7 as a function of exposure at 300 K, where the dotted lines represent the saturation of chemisorption.

preferentially grows, suggesting its physisorption nature. C 1s spectra also present a similar evolution as a function of pyrazine dosage. When the dosage is below 0.5 L, the main feature is the peak at 285.8 eV. At a high exposure of 8.0 L, the 286.6-eV peak dominates the spectra, attributable to physisorbed pyrazine. The BE of the N 1s and C 1s core level for physisorbed pyrazine on Si(111)-7 × 7 is in excellent agreement with the results of condensed pyrazine on Au.[28] Compared to the value (284.7 eV) of physisorbed benzene,[29] the higher C 1s BE of 286.6 eV observed for physisorbed pyrazine is due to the effect of the more electronegative N atoms incorporated in the aromatic ring.

To unambiguously assign these peaks, chemisorbed monolayer was obtained by annealing the multilayer pyrazine-covered surface (8.0 L) to 300 K to drive away all physisorbed molecules. Chemisorbed pyrazine gives a N 1s peak (Figure 4h) centered at 399.0 eV. Its narrow fwhm of ∼1.4 eV, close to the overall resolution of our XPS spectrometer, suggests that the two N atoms in chemisorbed pyrazine are chemically indistinguishable. Compared with the value of 400.6 eV observed for physisorbed pyrazine, the chemisorption on Si-(111)-7 × 7 results in a significant downshift of 1.6 eV in the BE of N (1s). The large shift implies the possible involvement of the nitrogen atoms in direct bonding to the surface reactive sites. A similar trend was previously observed for $CH_3-N=N-CH_3$ on Si surfaces, N 1s BE changing from 400.8 eV for physisorbed molecules to a value of 399.0 eV for chemisorbed state with direct Si−N bond formation.[30]

Figure 5h shows the corresponding C 1s spectrum for pyrazine chemisorbed on Si(111)-7 × 7. A single peak at 285.8 eV can be readily resolved, suggesting the existence of only

one chemically distinguishable form of carbon in chemisorbed species. This C 1s peak (285.8 eV) is noticed to be ~1.2 eV higher than the value of 284.6 eV observed for the C atom directly linked to surfaces through the Si−CH_2− group.[31,32] Its downshift of 0.8 eV from the value (286.6 eV) of physisorbed molecules can be attributed to the increase of electron density on these carbon atoms upon chemisorption. Pyrazine binds to an adjacent pair of adatom−rest atom through its two para nitrogen atoms, forming N−Si linkages. The chemisorption process is expected to destroy the ring π bond or aromaticity. This blocks the electron-withdrawing effect of nitrogen atoms through π bonding, subsequently enhancing the electron density of carbon atoms and resulting in a downshift in C 1s in chemisorbed pyrazine compared to physisorbed molecules.

The inset of Figure 5 presents the ratio of A_{C1s}/A_{Si2p} as a function of pyrazine exposure at room temperature. The value for each point was obtained by averaging three separate measurements to reduce possible errors. A_{C1s} is the C 1s peak area of chemisorbed pyrazine at 300 K. The saturation of the A_{C1s}/A_{Si2p} ratio indicates the completion of chemisorption. To estimate its absolute saturation coverage, XPS measurements for pyrazine-saturated Si(111)-7 × 7 are compared to those of chemisorbed benzene. The peak-area ratio, (A_{C1s}/A_{Si2p}) for pyrazine-saturated Si(111)-7 × 7 is 0.301. A value of 0.488 was found for chemisorbed benzene, which corresponds to an absolute coverage of 0.42 (the ratio between the reacted adatoms and the total adatoms on Si(111)-7 × 7).[33] After considering the numbers of carbon atoms in these two molecules, the saturation coverage, $\theta_{pyrazine}$, is estimated to be ~0.39 (0.42 × 0.301/0.488 × 6/4). This value approximately corresponds to 5 pyrazine molecules/unit cell.

III.C. DFT Calculations. In general, there are five possible ways for pyrazine to bind on Si(111)-7 × 7: (a) the interaction of lone-pair electrons at its N atom with the Si dangling bond to form a dative bond, similar to the case of pyridine on Si(100)[13] or Si(111)-7 × 7;[11] (b) [2 + 2]-like cycloaddition through a C═N bond; (c) typical [2 + 2]-like cycloaddition through a C═C; (d) [4 + 2]-like cycloaddition through two carbon atoms of the C═C−N═C; and (e) [4 + 2]-like cycloaddition through two nitrogen atoms of the N═C−C═N skeleton. DFT theoretical calculations were carried out to obtain the optimized geometric structures and energies for these possible adsorption configurations.

In modeling, a Si cluster of $Si_{30}H_{28}$ was cut from the central part of MMFF94-optimized[34] cluster, where the precision of atomic positions suffers the least from boundary effects. It contains an adatom and an adjacent rest atom from an unfaulted subunit, serving as a "di-σ" binding site for the attachment of one pyrazine molecule. Capping H atoms at the cluster boundaries are kept frozen. Silicon atoms in the bottom double layers are placed at bulk lattice positions prior to the geometry optimization process, with each Si−Si bond length set to 2.3517 Å and all bond angles adjusted to 109.4712°. A smaller structure of Si_9H_{12} was obtained from further reduction of $Si_{30}H_{28}$. Similarly, all capping H atoms were frozen during geometry optimization. Clusters corresponding to the six possible binding models were constructed by pyrazine adsorption onto the mother cluster (Si_9H_{12}). These Si clusters were previously used in successful prediction of the adsorption energy of benzene on Si(111)-7 × 7.[35]

Calculations were performed using the SPARTAN package.[36] The formation heats of chemisorbed configurations were calculated at the DFT theory level using the perturbative Beck−Perdew functional (pBP86) in conjugation with a basis set of DN** (comparable 6−31 G**).[36] Geometric optimizations were conducted under SPARTAN default criteria. Adsorption energy, synonymous to formation heat, is quoted here as the difference between the energy of the adsorbate/substrate complex and the total sum of the substrate and gaseous molecule. Figure 6 presents the six optimized geometries of the local minima for the $C_4H_4N_2/Si_9H_{12}$ model system. Their adsorption energies are given in Table 2. The calculation result reveals that the [4 + 2]-like cycloadditions are thermodynamically favored compared to the dative bonding and the [2 + 2]-like cycloadditions. Cluster $[4 + 2]_2$ (Figure 6f) is seen to be most stable, which is consistent with the observation of only the [4 + 2]-like reaction through two para nitrogen atoms in our experiments. The absence of the binding configuration of Mode IV (Figure 6e) through the two opposite carbon atoms in our experiments can be reasonably explained: (a) The Si−N bond is much stronger than the Si−C bond. The calculation result reveals that the [4 + 2]-like cycloaddition through two nitrogen atoms (33.3 kcal mol^{-1}) is thermodynamically favored compared to the [4 + 2]-like reaction through two carbon atoms (29.5 kcal mol^{-1}). (b) The selectivity of the attachment through the nitrogen atoms may also be attributable to the electrostatic interaction between the electron-rich nitrogen atom and the partially positively charged adatom. This attractive interaction lowers the transition state and directs the attachment of the nitrogen atom onto the adatom and consequently the molecule onto an adatom−rest atom pair. Thus, the [4 + 2]-like reaction through two para nitrogen atoms is thermodynamically and kinetically preferential with the formation of di-σ N−Si linkages. In addition, the calculated vibrational frequencies (Table 1) of the most stable intermediate, Cluster $[4 + 2]_2$ (Figure 6f), are consistent with our experimental vibrational spectrum.

IV. Discussion

The structural and electronic diversities of active sites on Si(111)-7 × 7 provide opportunities and flexibility for the covalent attachment of various functional organic molecules.[37,38] Previous studies on the reactivity and selectivity of six-membered aromatic molecule and five-membered heterocyclic aromatic molecules have suggested the [4 + 2]-like cycloaddition mechanism for benzene[9,10] and thiophene[6] Si(111)-7 × 7. In the case of furan, [7] additional surface-mediated dimerization reaction was evidenced. Our recent studies show that pyridine can bind to Si(111)-7 × 7 through two pathways, the dative bonding with electron transferring from the N atom of pyridine to a Si adatom and the [4 + 2]-like cycloaddition via the N atom and opposite C atom and an adjacent pair of adatom−rest atom.[11] The conversion from the dative bonding to di-σ binding configuration can be thermally promoted.

Pyrazine contains two N atoms positioned "para" to each other. As mentioned earlier, in section III.C., there are five possible ways for pyrazine to bind onto Si(111)-7 × 7. The corresponding surface reactions are schematically described in Figure 7. One possibility (reaction 1) is an end-on binding mode in which the lone-pair electrons on the nitrogen atom interacts with the Si surface dangling bond to form a dative bond, similar to the adsorption of $(CH_3)_3N$[39] and pyridine on Si(100)[13] or Si(111)-7 × 7.[11] Upon dative bonding, an unusually high BE (>401.5 eV) of the N 1s core level, significantly upshifted (~2.0 eV) compared to the value of physisorbed molecules, would be expected due to the partial transferring of lone-pair electron density from the N atom to the silicon surface atom. However, our observation of a significant downshift of 1.6 eV in N 1s for chemisorbed pyrazine excludes the possibility of this charge-

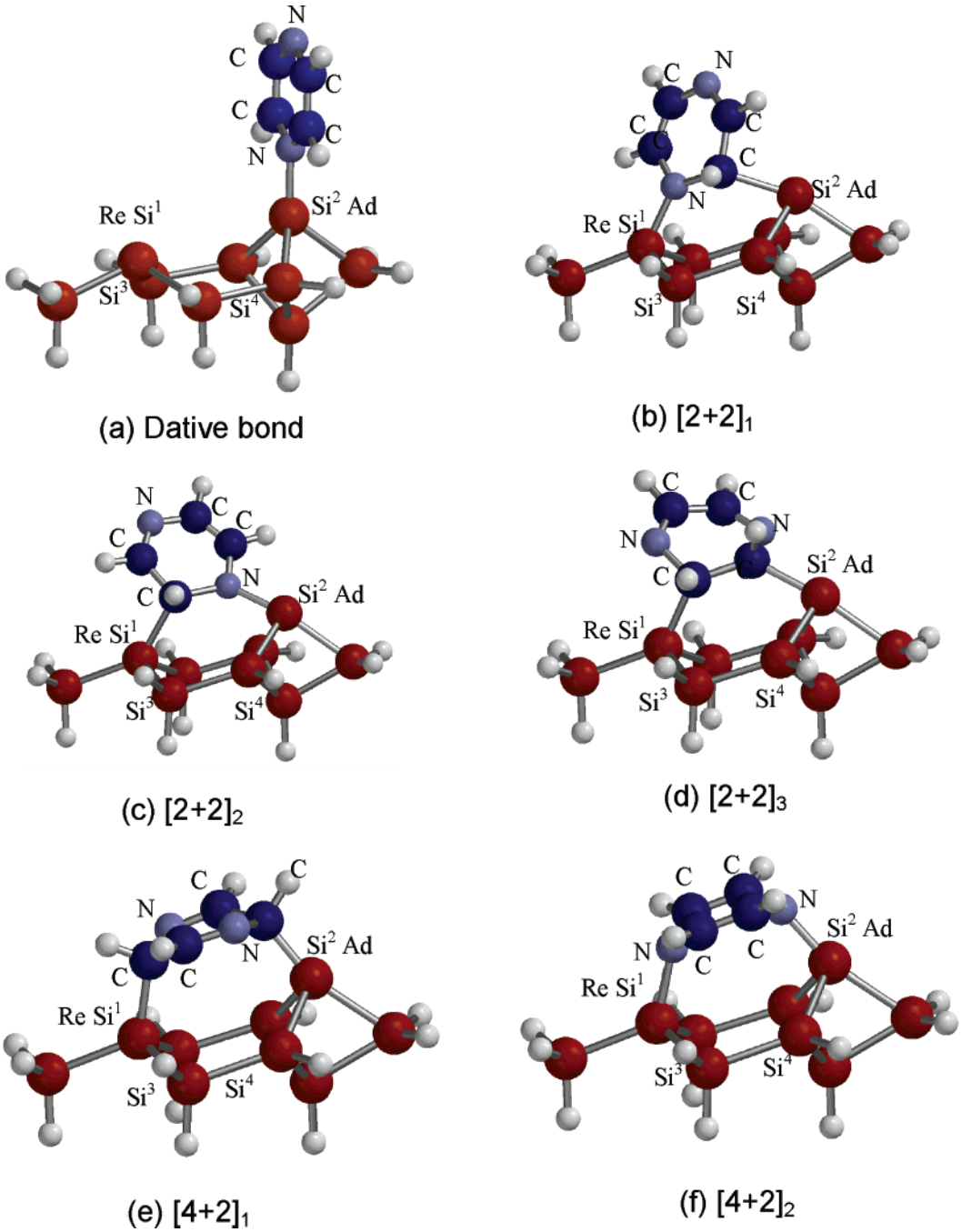

Figure 6. Optimized $C_4H_4N_2/Si_9H_{12}$ clusters corresponding to the six possible attachment modes through dative bond, [2 + 2]-like, and [4 + 2]-like addition reactions.

TABLE 2: Adsorption Energies of the Local Minima in the $C_4H_4N_2/Si_9H_{12}$ Model System from PBP/DN

reaction model	dative bond	$[2+2]_1$	$[2+2]_2$	$[2+2]_3$	$[4+2]_1$	$[4+2]_2$
adsorption energy[a]	14.2	23.46	8.43	0.14	29.46	33.29

[a] Adsorption energy: $\Delta E = [E(Si_9H_{12}) + E(C_4H_4N_2)] - E(C_4H_4N_2/Si_9H_{12})$. All energies are in kcal mol^{-1}.

transfer complex. In the [2 + 2]-like (reactions 2 and 3) and [4 + 2]-like (reaction 4) cycloadditions through C═C, C═N, and C═N−C═C skeletons, the hybridization of one or more ring C atoms from sp^2 to sp^3 would be expected. In our vibrational studies, the retention of the sp^2 configuration for all four carbon atoms in the chemisorbed intermediate was evidenced in the detection of only one (sp^2) C−H stretching at 3071 cm^{-1} without any intensity at 2900 cm^{-1} for (sp^3) C−H stretching. This clearly rules out the possibility for these three reactions. In fact, our experimental and theoretical results are consistent with the [4 + 2]-like cycloaddtion through two para nitrogen atoms (reaction 5). In the resulting 1,4-*N*,*N*-dihydropyrazine-like adduct, two N−Si σ linkages are formed together with two isolated C═C bonds, retaining sp^2 configuration for carbon atoms. Indeed, our HREELS results show that, upon chemisorption, all the vibrational modes related to (sp^2) C−H remain unchanged together with the appearance of unconjugated C═C vibrational feature at 1615 cm^{-1}. Thus, our vibrational observation strongly suggests that pyrazine covalently bonds to the adjacent adatom and rest atom on Si(111)-7 × 7 through two para nitrogen atoms to form di-Si−N-σ via the [4 + 2]-like cycloaddition mechanism. This is also in good agreement with the XPS results and the prediction of DFT calculations.

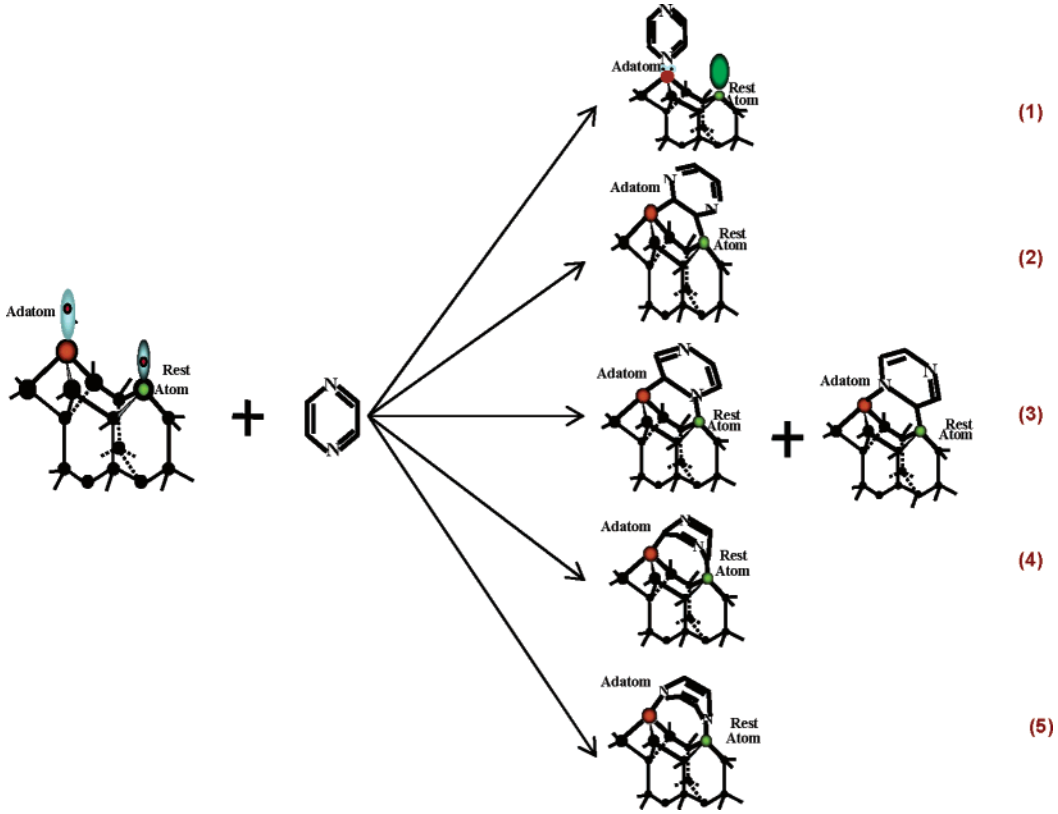

Figure 7. Schematic diagram for the possible reactions of pyrazine on Si(111)-7 × 7.

TABLE 3: XPS N (1s) Binding Energy (eV) for Adsorption of N-Containing Molecules on Si Surface, Forming the Si−N σ Bond

molecule	physisorption	chemisorption	downshift
NH_3 on Si(111)[40]	400.1	398.5	1.6
pyrrole on Si(111)[8]	400.4	399.3	1.1
phenyl isothiocyanate on Si(100)[41]	400.2	398.5	1.7
azo-*tert*-butane on Si(100)[30]	400.8	399.0	1.8
pyridine on Si(111)[11]	400.0	398.8	1.2
pyrazine on Si(111)−7 × 7[a]	400.6	399.0	1.6

[a] Present work.

In our XPS studies of chemisorbed molecules, the BE of N 1s of chemisorbed pyrazine displays large shift of 1.6 eV from that of physisorbed multilayer, which implies that direct involvement of N atoms in pyrazine binding on Si(111)-7 × 7. As shown in Table 3,[8,11,30,40−41] the N (1s) BE of 399.0 eV for pyrazine on Si(111)-7 × 7 coupled with the downshift (1.6 eV) is in good agreement with results obtained for other molecules covalently attached to the silicon surface through the direct bonding of their N atoms with the Si surface reactive sites.

Chemisorbed pyrazine gives a single C 1s peak at 285.8 eV, downshifted by 0.8 eV from that of physisorbed multilayer (286.6 eV). This BE is in fact nearly 1.2 eV higher than the value (284.6 eV) found for the Si−C σ linkages.[31,32] Thus, the C 1s intensity observed for chemisorbed pyrazine cannot be attributed to the C atoms bonding with the surface Si atoms. The fact of observing the 0.8 eV downshift for the C 1s core level can be explained considering the structural changes and electron redistribution in chemisorbed pyrazine depicted in the theortical model (Figure 6f). The attachment of two para-nitrogen atoms to the adjacent adatom and rest atom significantly tilts the molecular plane and removes the aromaticity. As a result, the π-electron polarization toward the nitrogen atoms occurring in physisorbed pyrazine does not exist in chemisorbed state. This enhances the relative electron density at the carbon atoms in the resulting 1,4-*N*,*N*-dihydropyrazine-like surface intermediate, subsequently lowering the C 1s BE. This is consistent with our experimental conclusion that pyrazine selectively binds on the Si(111)-7 × 7 through two para-nitrogen atoms with the adjacent adatom and rest-atom.

In contrast to the pyridine/Si(111) system, there is no observation of the formation of dative bonds for pyrazine chemisorbed on Si(111)-7 × 7. The absence of dative bonds for pyrazine/Si(111) can be reasonably explained by the following: (a) Pyridine molecule is a stronger electron donor. The electron density at the nitrogen atom in pyridine is higher than that in pyrazine, as evidenced by the lower BE of N 1s core level for physisorbed pyridine (400.0 eV) as compared to that for physisorbed pyrazine (400.6 eV). (b) The dative bond for pyridine/Si(111) is more stable. DFT calculations show that the BE of the dative bond for pyrazine/Si(111) is lower than that for pyridine/Si(111) by 12.2 kcal/mol. Moreover, compared to the dative bonded state, the 1,4-*N*,*N*-dihydropyrazine-like binding configuration is thermodynamically favorable by 19 kcal/mol. However, for the pyridine/Si(111) system, the BE of dative-bonded product (26.4 kcal/mol) is comparable to that of the [4 + 2]-like addition product (26.7 kcal/mol). This is consistent with the high selectivity observed in pyrazine binding on Si(111)-7 × 7 through the di-σ N−Si linkages.

V. Conclusions

Both experimental results and theoretical calculation show that pyrazine interacts with the Si(111)-7 × 7 surface through a [4 + 2]-like cycloaddition reaction between two para nitrogen atoms and an adjacent adatom−rest atom pair to form two new Si−N σ bonds. The cycloadduct containing two unconjugated C═C double bonds may be employed as an intermediate to synthesis in a vacuum via reacting with chosen organic

functionalities through typical vinyl reactions including addition, cyanoethylation, and polymerization or be used as a precursor for further modification of Si surface.

References and Notes

(1) Yates, J. T., Jr. *Science* **1998**, *279*, 335−336.

(2) Hamers, R. J.; Coulter, S. K.; Ellison, M. D.; Hovis, J. S.; Padowitz, D. F.; Schwartz, M. P.; Greenlief, C. M.; Russell, J. N., Jr. *Acc. Chem. Res*. **2000**, *33*, 617−624.

(3) Wolkow, R. A. *Annu. Rev. Phys. Chem.***1999**, *50*, 413−441.

(4) Takayanagi, K.; Tanishiro, Y.; Takahashi, M.; Takahashi, S. *J. Vac. Sci. Technol*. **1985**, *3*, 1502−1506.

(5) Chadi, D. J.; Bauer, R. S.; Williams, R. H.; Hansson, G. V.; Bachrach, R. Z.; Mikkelsen, J. C., Jr.; Houzay, F.; Guichar, G. M.; Pinchaux, R.; Petroff, Y. *Phys. Rev. Lett*. **1980**, *44* (12), 799−802.

(6) Cao, Y.; Yong, K. S.; Wang, Z. Q.; Chin, W. S.; Lai, Y. H.; Deng, J. F.; Xu, G. Q. *J. Am. Chem. Soc*. **2000**, *122*, 1812−1813.

(7) Cao, Y.; Wang, Z. H.; Deng, J. F.; Xu, G. Q. *Angew. Chem., Int. Edit.* 2000, **39**, 2740−2743.

(8) Yuan, Z. L.; Chen, X. F.; Wang, Z. H.; Yong, K. S.; Cao, Y.; Liu, Q. P.; Xu, G. Q. *J. Chem. Phys.* **2003**, *119*, 10389−10395.

(9) Carbone, M.; Piancastelli, M. N.; Casaletto, M. P.; Zanoni, R.; Comtet, G.; Dujardin, G.; Hellner, J. L. *Phys. Rev. B* **2000**, *61*, 8531−8536.

(10) Cao, Y.; Wei, X. M.; Chin, W. S.; Lai, Y. H.; Deng, J. F.; Bernasek, S. L.; Xu, G. Q. *J. Phys. Chem. B* **1999**, *103*, 5698−5702.

(11) Tao, F.; Lai, Y. H.; Xu, G. Q. *Langmuir* **2004**, *20*, 366−368.

(12) Billes, F.; Mikosch, H.; Holly, S. *THEOCHEM* **1998**, *423*, 225−234.

(13) Tao, F.; Qiao, M. H.; Wang, Z. H.; Xu, G. Q. *J Phys. Chem. B* **2003,** *107* 6384−6390.

(14) Avouris, P.; Demuth, J. E. *J. Chem. Phys*. **1981**, *75*, 4783−4794.

(15) Hallmark, V. M.; Campion, A. *J. Chem. Phys*. **1986**, *84*, 2933−2941.

(16) Otto, A.; Reihl, B. *Surf. Sci*. **1986**, *178*, 635−645.

(17) Dudde, R.; Frank, K. H.; Koch, E. E. *J. Electron. Spectrosc. Relat. Phenom*. **1988**, *47*, 245−255.

(18) Hamm, U. W.; Lazarescu, V.; Kolb, D. M. *J. Chem. Soc., Faraday Trans*. **1996**, *92* (20), 3785−3790.

(19) Tao, F.; Wang, Z. H.; Qiao, M. H.; Liu, Q.; Sim, W. S.; Xu, G. Q. *J. Chem. Phys.* **2001**, *115*, 8563−8569.

(20) Hewett, K. B.; Shen, M. H.; Brummel, C. L.; Philips, L. A. *J Chem. Phys*. **1993**, *100* (6), 4077−4086.

(21) Zarembowitch, J.; Bokobza-Sebagh, L. *Spectrochim. Acta, Part A* **1976**, *32A*, 605−615.

(22) Stidham, H. D. *Spectrochim. Acta* **1965**, *21*, 23−32.

(23) Cao, Y.; Yong, K. S.; Wang, Z. H.; Deng, J. F.; Lai, Y. H.; Xu, G. Q. *J. Chem. Phys.* **2001**, *115*, 3287−3296.

(24) Daimay. L. V.; Norman, B. C.; William, G. F.; Feanette, G. G. *The handbook of Infrared and Raman Characteristic Frequencies of Organic Molecules*; Academic Press: Boston, **1991**.

(25) Bu, Y.; Lin, M. C. *Surf. Sci.* **1994**, *311*, 385−394.

(26) Qiao, M. H.; Cao, Y.; Deng, J. F.; Xu, G. Q. *Chem. Phys. Lett.* **2000**, *325*, 508−512.

(27) Chabal, Y. J.; Raghavachari, K. *Phys. Rev. Lett*.**1984,** *53*, 282−285.

(28) Clark, D. T.; Chambers, R. D.; Kilcast, D.; Musgrave, W. K. R. *J. Chem. Soc., Faraday Trans.* **1972**, *68* (2), 309−319.

(29) Moulder, J. F.; Stickle, W. F.; Sobol, P. E.; Bomben, K. D. *Handbook of X-ray Photoelectron Spectroscopy*; Chastain, J., Ed.; Perkin-Elmer Corp.: Eden Prairie, MN, 1992.

(30) Ellison, M. D.; Hovis, J. S.; Liu, H. B.; Hamers, R. J. *J. Phys. Chem. B* **1998**, *102*, 8510−8518.

(31) Schwartz, M. P.; Hamers, R. J. *Surf. Sci*.**2002**,*515*, 75−86.

(32) Tao, F.; Sim, W. S.; Xu, G. Q.; Qiao, M. H. *J. Am. Chem. Soc*. **2001**, *123*, 9397−9403.

(33) Taguchi, Y.; Fujisawa, M.; Nishijima, M. *Chem. Phys. Lett*. **1991**, *178*, 363−368.

(34) Halgren, T. A. *J. Comput. Chem*. **1996**, *17*, 490−519.

(35) Wang, Z. H.; Cao, Y.; Xu, G. Q. *Chem. Phys. Lett*. **2001**, *338*, 7-13.

(36) Hehre, W. J.; Yu, J.; Klunzinger, P. E.; Lou, L. *A Brief Guide to Molecular Mechanics and Quantum Chemical Calculation*; Wavefunction: Irvine, CA, 1998.

(37) Tao, F.; Dai, Y. J.; Xu, G. Q. *Phys. Rev. B* **2002**, *66*, 035420/1−035420/6.

(38) Rochet, F.; Jolly, F.; Bournel, F.; Dufour, G.; Sirotti, F.; Cantin, J. L. *Phys. Rev. B* **1998**, *58*, 11029−11042.

(39) Cao, X. P.; Hamers, R. J. *J. Am. Chem. Soc*. **2001**, *123*, 10988−10996.

(40) Bozso, F.; Avouris, P. *Phys. Rev. B* **1988**, *38*, 3937−3942.

(41) Ellison, M. D.; Hamers, R. J. *J. Phys. Chem. B* **1999**, *103*, 6243−6251.